Label-free enzyme sensing with grated silicon photonic wire

L.J. Kauppinen, M. Dijkstra, H.J.W.M. Hoekstra, and R.M. de Ridder

University of Twente, MESA$^+$ Institute for Nanotechnology, 7500 AE Enschede, The Netherlands

We have investigated the label-free biosensing properties of grated silicon photonic wire (GSPW) waveguides with cross-sectional dimensions of 350 nm x 220 nm, fabricated using a 248-nm deep UV lithography process. The steep edges of the optical transmission spectrum of the GSPW enable detection of very small spectral shift, hence of small index changes.

To obtain an antibody layer for the biosensing experiment, an immobilization process is required. We followed the standard immobilization process developed by Imenz B.V. The antibody immobilization process and the binding process of enzymes on an immobilized antibody layer have been monitored with the GSPW based sensor.

Introduction

An important application field of integrated optical (IO) sensors is label-free bio-sensing, in which certain bio-molecules are selectively captured by a thin layer of receptor molecules, e.g., antibodies, attached to the surface of the IO sensor [1-2]. Hereby, sensing is based on the detection of small structural changes in the ambient environment of the waveguide by the evanescent tail of the light outside the waveguiding structure. Due to the exponential nature of the evanescent field, the sensor will only respond to changes in composition of the thin surface layer, which leads to high spatial selectivity on sensing the molecular species attached to the surface.

We have studied the properties of a grated silicon photonic wire (GSPW) for biosensing applications. Due to the sharp spectral features of a grating, high sensitivity is anticipated [3-4].

We have monitored the binding process of enzymes on an immobilized antibody layer, that we applied to the surface of a GSPW sensor, as well as part of the antibody immobilization process.

Materials and methods

The GSPWs have been fabricated using the standard 248-nm deep-UV lithography process for photonic crystals and photonic wire established at IMEC, Leuven [5]. The grating structure has been realized by periodically varying the width of the waveguide as shown in the Fig. 1. Fabrication process specifications imply a Si-layer thickness of 220 nm, and a minimum grating period of 450 nm.

The dimensions of the wide (width w) and narrow (width d) segments were chosen such that the photonic stopband would be in the 1.5 μm wavelength region. Due to the geometry of the photonic wire, only three-dimensional calculations would provide realistic information on the transmission properties [6]. However, on designing we used a two-dimensional method in which we used a modesolver to calculate effective refractive indices for the wide and narrow segments. Based on the calculated effective indices it was possible to use Bragg's equation to calculate the stopband position. In view of our experimental data, this fast method appeared to be fairly accurate in

predicting the stopband positions; all of the stopbands were within a ~30 nm wavelength range from the target value.
Due to the properties of the used photolithographic process, the actual grating shape is different from the designed one, as shown in the Fig. 2. The rectangular shape is smoothened to a sinusoidal like shape. Nevertheless, we have measured pronounced stopbands for all of these gratings.

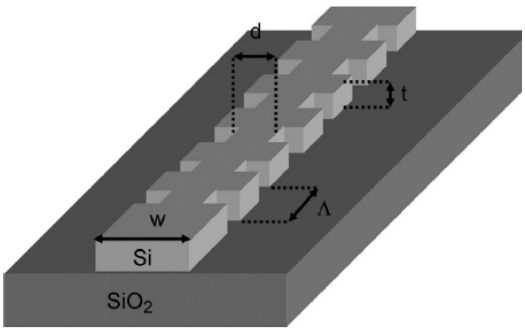

Fig 1. Lay-out of a grated silicon photonic wire. Waveguide widths *w* and *d* are of the order of 400-300 nm, Λ=450 nm and the waveguide thickness *t* is 220 nm.

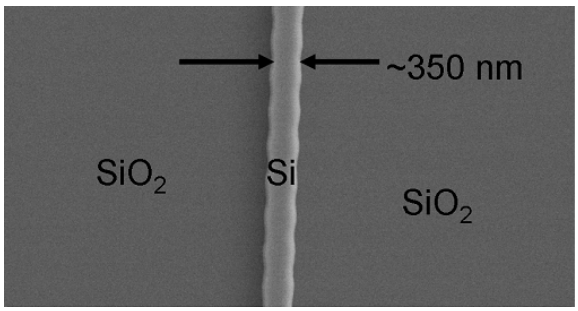

Fig 2. SEM image of 350 nm wide grated photonic wire. Lithography smoothens the rectangular shape.

In a label-free biosensing scheme, the molecules that bind to the surface of the waveguide will cause a change in the cladding index. At the stopband edge the change in the transmitted power T is in first order approximation directly proportional to the change in cladding index n_{clad} according to:

$$\Delta T \approx 2\eta\Lambda \frac{\partial T}{\partial \lambda} \Delta n_{clad}, \quad (1)$$

in which Λ is the period of the grating and η is the fraction of energy density in the cladding. Therefore, a steep stopband edge (high $\partial T/\partial\lambda$) and a large energy density fraction in the cladding (η) will result in high sensitivity to cladding-index changes. The detection limit of the sensor depends on how accurately the small power change ΔT can be measured.
To obtain an antibody layer for the bio-sensing experiment, an immobilization process is required. We followed the standard immobilization process developed by Imenz b.v. This process consists of five main steps as shown in Fig 3. The first two steps were performed in a cleanroom. The remaining three steps were performed while monitoring the spectral response of the GSPW.

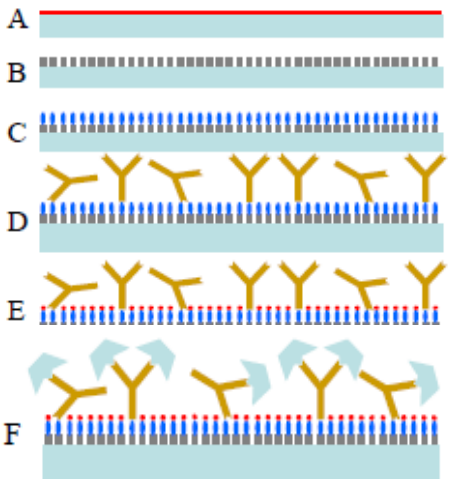

Fig 3. Immobilization process (A-E) and enzyme binding (F). (A) Surface cleaning and activation, (B) silanization, (C) glutaraldehyde, (D) antibody immobilization, and (E) blocking of reactive carbonyl groups.

Monitoring the immobilization process and enzyme binding

As a demonstration of label-free bio-sensing, we performed an experiment in which we immobilized an antibody layer on the waveguide, following the procedure shown in Fig 3, and then measured the reaction as enzymes became attached to to the anti-bodies. The sensor was also used to monitor part of the immobilization process.

Initially, we measured the stop-band position of the GSPW after the silization. In this case, the GSPW sensor is covered by a monolayer of silane, and then air. Next, a PBS solution was flowed into the cuvette. This solution replaces air as the top cladding, and a stopband shift of approximately 45 nm was observed. We measured the refractive index of the PBS solution using an Abbe refractometer (n=1.3348). The stopband shift was roughly 10 nm smaller than expected from a bulk index sensing experiment we reported previously [4]. This indicates that the sensor had become less sensitive to bulk index changes after silanization. This, in turn, could mean that silanization had formed a thicker silane layer than just the desired monolayer.

After the PBS solution, a glutaraldehyde solution was flowed into the cuvette to form a surface for the anti-bodies to attach to. As the glutaraldehyde solution has a higher refractive index (n=1.3480) than the PBS, we expected the shift in the stop-band position to continue. Surprisingly, the shift was in the "wrong" direction: into a lower wavelength region. We have measured the same unexpected stopband shift several times. The reaction time for the glutaraldehyde process step is 1 hour. During this time, we noticed a stopband shift of few nanometres, back to higher wavelengths. PBST (n=1.3345) was flowed in as an intermediate step; however the stopband position remained at about 30 nm shorter wavelength than before the glutaraldehyde step.

Antibodies, selective to an enzyme known as PepN, were immobilized on the glutaraldehyde surface by flowing an antibody solution into the cuvette. The reaction time for this step is specified as one hour at 37 ^{0}C; however, to avoid complications due to the thermo-optic effect, we performed the step at room temperature (19 ^{0}C) but with a longer reaction time of 1.5 hours. We measured deformed stopband shapes while the antibody solution was in a cuvette. One possible reason for this is that clustering of the antibody molecules near the surface may destroy the uniformity of the grating.

The blocking solution restored the shape of the spectrum. Also, a slight shift to the higher wavelengths was observed, indicating an index increase due to both immobilized antibodies and the attached blocking molecules.

PepN enzyme binding on the antibody interface was monitored by measuring the transmittance at a couple of operation wavelengths near the stopband edge. The specified reaction time for enzyme binding is one hour. Based on measurement results, the enzyme binding appears to be active during the first 30 minutes,

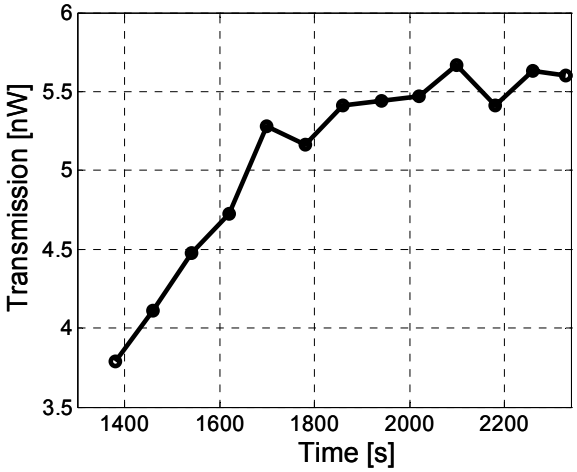

Fig 4. Measured reaction curve of enzyme binding process. A saturation in the binding process happens after a reaction time of 30 minutes.

after which the activity falls to a lower level. Figure 4 shows the last 15 minutes of the enzyme binding reaction curve. The binding curve is clearly saturated at the end.
The total wavelength shift caused by the enzyme binding is approximately 230 pm, which corresponds to bulk index change of ~10^{-3}. This index change is high, and given the sensor's detection limit of 10^{-5}, 100 times smaller enzyme concentrations can potentially be detected. Due to the compact size of the GSPW sensor, the sample volume can be very small, down to the picolitre level.

Conclusions

Biosensing using a GSPW sensor has been demonstrated by immobilizing the enzyme antibody interface on a surface of the sensor. Enzyme binding on this interface has been measured. The sensor was also used to monitor the immobilization process.

Acknowledgements

This research is supported by the Dutch Technology Foundation STW, applied science division of NWO and the Technology Program of the Ministry of Economic Affairs

References

[1] K. De Vos, J. Girones, S. Popelka, E. Schacht, R. Baets, and P. Bienstman, "SOI optical microring resonator with poly(ethylene glycol) polymer brush for label-free biosensor applications," *Biosens. Bioelectron.*, vol. 24, pp. 2528–2533, 2009.

[2] G. Rong, A. Najmaie, J.E. Sipe, and S.M. Weiss, "Nanoscale porous silicon waveguide for label-free DNA sensing," *Biosens. Bioelectron.*, vol. 23, pp. 1572–1576, 2008.

[3] W.C.L. Hopman, P. Pottier, D. Yudistira, J. van Lith, P.V. Lambeck, R.M. De La Rue, A. Driessen, H.J.W.M. Hoekstra, and R.M. de Ridder, "Quasi-one-dimensional photonic crystal as a compact building-block for refractometric optical sensors, *IEEE J. Sel. Top. Quantum Electron.*, vol. 11, pp. 11-16, 2005.

[4] L.J.Kauppinen, H.J.W.M. Hoekstra, and R.M. de Ridder, "A compact refractometric sensor based on grated silicon photonic wires," *Sens. Actuators, B*, vol. 139, pp. 194-198, 2009

[5] Silicon Photonics Platform, http://www.epixfab.eu/

[6] M. Gnan, G. Bellanca, H.M.H. Chong, P. Bassi, and R.M. de la Rue, "Modelling of photonic wire Bragg gratings", *Opt. Quantum Electron.*, vol. 38, pp. 133–148, 2006.